H + O_2 + M (=N_2, H_2O, Ar) Three-Body Rate Coefficients at 298–750 K

Karen L. Carleton, William J. Kessler, and William J. Marinelli*

Physical Sciences Inc., 20 New England Business Center, Andover, Massachusetts 01810

Received: November 23, 1992; In Final Form: March 30, 1993

Three-body rate coefficients for reactions of H + O_2 + M where M = N_2 and H_2O have been measured in a high-temperature flow reactor as a function of temperature up to 750 K. Room-temperature rate coefficients for M = Ar have also been quantified. The rate coefficients are measured by the flash photolysis method where atomic hydrogen is produced by excimer laser photolysis of precursor molecules (H_2S or H_2O) and then probed by either laser-induced fluorescence or resonance absorption. The rate coefficient measurements for nitrogen (298–580 K) can be described by the Arrhenius expression $k_{N_2} = (2.9 \pm 0.8) \times 10^{-33} \exp[(825 \pm 130)/T]$ cm^6 molecule^{-2} s^{-1}. Rate coefficients measured for water are $k_{H_2O}(575) = (1.2 \pm 0.3) \times 10^{-31}$, $k_{H_2O}(650) = (1.0 \pm 0.3) \times 10^{-31}$, and $k_{H_2O}(750) = (1.2^{+0.9}_{-0.6}) \times 10^{-31}$ cm^6 molecule^{-2} s^{-1}. Room-temperature measurements for Ar gave a rate coefficient of $k_{Ar}(298) = (2.1 \pm 0.2) \times 10^{-32}$.

1. Introduction

Three-body reactions are important in combustion processes because of their ability to remove chain-propagating species. The energy of recombination released as a result of the formation of stable products provides the desired thrust in propulsion systems. This may happen directly or via the formation of radical intermediates which participate in other terminating reactions. The current study was performed because of renewed interest in rate coefficients for the H_2/O_2 combustion system in hypersonic scramjet applications. In these engines, the gas residence times are short and temperature and pressure are changing rapidly. Under these conditions, many of the three-body reactions are slow and hence may not achieve equilibrium. Accurate values of the three-body rate coefficients for the important reactions must be known in order to optimize combustor performance.[1]

In the H_2/O_2 combustion system, the important three-body reactions as recognized from studies on flame propagation and explosion limits are[2,3]

$$\begin{aligned} H + O_2 + M &\rightleftharpoons HO_2 + M \\ H + OH + M &\rightleftharpoons H_2O + M \\ H + H + M &\rightleftharpoons H_2 + M \\ H + O + M &\rightleftharpoons OH + M \end{aligned} \qquad (1)$$

where M refers to the third body. Typically H_2, O_2, N_2, and H_2O are important third bodies for air-breathing systems. The wide range of rate coefficients measured for these reactions has been summarized in the reviews of Baulch et al.[4,5] The data show orders of magnitude discrepancies between reported results and a lack of reliable data for several important third bodies.

Recent measurements of the H + O_2 + M reaction rate coefficient have been made by the atmospheric chemistry community, where interest concerns the role of HO_x chemistry in ozone photochemical cycles. At 300 K, the most recent recommendation of the NASA JPL Panel[6] is a rate coefficient of approximately 5.7×10^{-32} cm^6 molecule^{-2} s^{-1} for air as the third body, which agrees with measurements with N_2 by Hsu et al.[7,8] While these results agree with the recommendations of Baulch et al.[5] within the error bars, the recommended values differ by 50% at 300 K. They also differ quite substantially from the work of Dixon-Lewis[2] who gave a rate coefficient of 2.5×10^{-32} cm^6 molecule^{-2} s^{-1} for an N_2 third body at 300 K. This value is consistent with the early Baulch review, which gave a rate coefficient of 2.2×10^{-32} cm^6 molecule^{-2} s^{-1}.[4]

Our experimental approach to measuring this rate coefficient employs the flash photolysis method for the generation of hydrogen atoms in the presence of oxygen. The decay of the H atom concentration is followed using either two-photon laser-induced fluorescence or Lyman–α resonance absorption spectroscopy. The H atom decay rates obtained from either method are analyzed first as a function of oxygen concentration and then as a function of total pressure to obtain the rate coefficient for the three-body reaction. We have studied several third bodies including N_2 at 298–580 K, Ar at 298 K, and H_2O between 575 and 750 K.

2. Experimental Section

In these experiments, we employed the pulsed photolysis of hydrogen sulfide (H_2S) or water (H_2O) at 193 nm to produce hydrogen atoms in the presence of excess O_2. For the excimer laser fluence and precursor species concentrations employed, the H atoms reacted with O_2 molecules under pseudo-first-order conditions. The H atom concentrations were measured by two different methods: two-photon laser-induced fluorescence (LIF) and resonant absorption of Lyman–α radiation. The time-resolved H atom first-order decays were studied as a function of pressure and temperature to obtain the rate coefficient for the three-body reaction between H atoms and O_2 to produce HO_2. Different aspects of the experimental apparatus are discussed below.

2.1. Flow Reactor. The experiments have been performed in two different high-temperature flow reactors. In the preliminary N_2 studies, a four-way stainless steel chamber with the fourth arm extended was used to preheat the gases flowing through the reactor. Most of the data have been taken in the second reactor, which is a large stainless steel six-way cross with a 5-cm-diameter quartz liner (Figure 1). Typical operating parameters were pressures of 50–500 Torr and temperatures of 300–800 K. Fast linear gas flow speeds (>10 cm s^{-1}) were used to ensure that the gas volume is swept out between laser pulses, eliminating secondary chemistry effects.

The gas temperature was measured by radiation-shielded thermocouples in the reaction zone and also quantified using NO LIF thermometry. In this case, the rotational temperature of NO was determined by a Boltzmann analysis of the NO A–X (2,0) spectrum from NO seeded into a flow of either N_2 or He. The radiation-shielded thermocouple and the NO thermometry gave temperatures which agreed to within 20 K (the error bars of the LIF thermometry technique).

2.2. H Atom Generation. Hydrogen atoms were generated by excimer laser photolysis of either H_2S or H_2O at 193 nm.

0022-3654/93/2097-6412$04.00/0

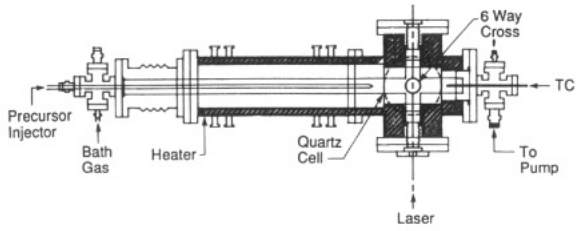

Figure 1. High-temperature flash photolysis reactor with quartz reaction cell.

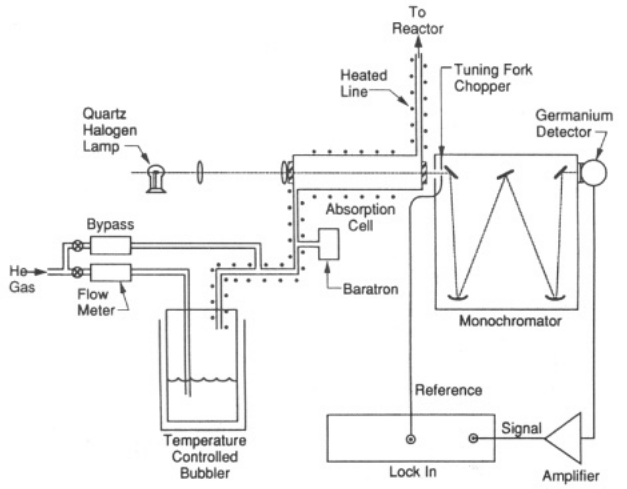

Figure 2. Water delivery system including temperature-controlled bubbler, absorption cell, and monochromator with infrared detector.

Hydrogen sulfide was used for the N_2 and Ar three-body studies. Photolysis laser fluences were approximately 50 mJ cm^{-2} for the LIF detection studies at 10-Hz repetition rates. The higher sensitivity of the Lyman–α resonance absorption detection scheme enabled the use of laser fluences as low as 10 mJ cm^{-2}.

To minimize H_2S heterogeneous decomposition on the hot reactor walls, H_2S was added through a water-cooled injector approximately 15 cm upstream of the photolysis zone. Minimal H_2S concentrations were required for these experiments (<0.03%). For the Lyman–α resonance absorption studies, less than 0.003% H_2S concentrations were required.

For the measurements of the H + O_2 + M reaction with H_2O as the third body, H_2O was also used as the precursor molecule for H atom production. Excimer photolysis of H_2O at 193 nm through hot band absorption[9,10] resulted in comparable H atom concentrations to those obtained using H_2S photolysis because of the large water concentrations used for these measurements. We have recently quantified the water absorption cross section at 193 nm using this reactor.[10] Water was introduced into the reactor by passing helium through a temperature-controlled saturator. Its flow rate was quantified by an infrared absorption flow monitor described previously (Figure 2).[10]

The water flow monitor system was calibrated by collecting the water in a liquid nitrogen cooled trap over a fixed period of time. The trap was weighed before and after collecting the water to quantify the average water flow rate during that time. The water flow rates determined by the trapping measurements were accurate to ±10% and were used to calibrate the absolute H_2O flow rates measured by IR absorption.

2.3. H Atom Detection. As mentioned, hydrogen atoms were detected by both two-photon LIF and Lyman–α resonance absorption. The two-photon LIF method was necessary for the H_2O third-body studies as H_2O has significant absorption at 121.6 nm. Both techniques and their experimental geometries for the rate coefficient measurements are described below.

Laser-Induced Fluorescence. The two-photon LIF technique has been demonstrated by several groups in the laboratory and in atmospheric pressure flames.[11-13] Two-photon absorption at 205.14 nm excites the ground-state ^2S H atoms to the $3d^2\ D_{5/2}$ and $3s^2\ S_{1/2}$ states, which then radiate on several lines within 0.1 nm of 656.2 nm.[14] The fluorescence observed at 656 nm is directly proportional to the H atom density, as was experimentally verified.

The 205-nm excitation wavelength was generated by doubling a Nd:YAG pumped dye laser (Rhodamine 640) and then mixing the doubled and fundamental light in a β-barium borate crystal to produce 1–2 mJ. This beam was either gently focused with a 1-m lens or telescoped to increase the final laser fluence. The excimer photolysis and LIF probe beams were counterpropagated through the photolysis cell. The photolysis laser beam area was kept larger than that of the probe laser to eliminate problems from H atom diffusion. The fluorescence was imaged onto a photomultiplier tube (PMT) through several filters including a 1-nm band-pass filter at 656 nm. The PMT signal was amplified, averaged using a gated boxcar signal averager, and recorded on a computer. The decay of the H atom concentration was recorded by collecting the LIF signal as a function of time following H_2S photolysis.

Resonance Absorption. The low sensitivity of the two-photon LIF technique necessitated the use of relatively large quantities of H_2S and high excimer laser fluences. Under these conditions, secondary chemistry of HS radicals produced from H_2S photolysis or O atoms produced by 193-nm photolysis of oxygen (see below) could complicate the kinetics. To reduce these effects, the N_2 three-body rate coefficients were also measured with Lyman–α resonance absorption. This sensitive technique allowed us to decrease both the H_2S concentrations and the excimer laser fluences by an order of magnitude.

The Lyman–α emission was produced by a 70-W microwave discharge of low-grade helium (1–2 Torr). The light was directed across the reactor, focused with a lens, spectrally filtered with a monochromator, and detected with a solar blind photomultiplier. A computer-controlled multichannel scaler coupled to an amplifier/disciminator was used to quantify the Lyman–α radiation intensity as a function of time after the photodissociation pulse. The excimer laser was introduced through the top port in the chamber and crossed the Lyman–α beam in the chamber center.

The H atoms were detected as a decrease in the Lyman–α emission from the lamp as a result of absorption by H atoms created by the excimer laser photolysis of H_2S. The H atom concentration was proportional to the absorbance:

$$[H(t)] \propto \ln(I_0/I(t)) \qquad (2)$$

The relative time-dependent H atom concentration was obtained from the time-resolved absorption signal. In past resonant absorption studies, controversies have arisen about the correspondence between absorption and concentration due to the mismatch between emission and absorption profiles. In these experiments, the H atom concentrations were experimentally verified to be linearly proportional to the H atom number densities generated in the reactor up to absorbances of 0.4 via quantitative photodissociation of H_2S.

2.4. Kinetic Measurements. The three-body rate coefficient measurements were performed by quantifying H atom decay rates under pseudo-first-order conditions. The O_2 partial pressure never exceeded 10% of the total pressure to minimize effects of varying third-body reaction efficiencies. Measurements were performed at fixed pressure for a range of O_2 concentrations and then repeated for a range of pressures. This process was repeated for each temperature measurement to determine the three-body rate coefficient. Temperature-dependent measurements were performed for N_2. Room-temperature three-body rate coefficients were measured for argon. Finally, temperature-dependent rate coefficients were measured for H_2O with He as a carrier gas. In the latter experiments, the He concentration was kept fixed while varying the H_2O concentrations. This was accomplished by

TABLE I: Kinetic Parameters for Rate Coefficients Included in H_2S Based Studies of $H + O_2 + N_2$

	A	n	B	ref[a]
1. $H + O_2 + M \rightarrow HO_2 + M$	6.5(-33)	0	680	1
2. $H + H_2S \rightarrow H_2 + HS$	1.3(-11)	0	-860	2
3. $H + HO_2 \rightarrow OH + OH$	3.6(-10)	0	-503	3
4. $O + HS \rightarrow SO + H$	1.6(-10)	0	0	2*
5. $O + H_2S \rightarrow OH + HS$	4.4(-12)	0	-1700	2
6. $H + HS \rightarrow H_2 + S$	6.7(-10)	0	-990	2*
7. $H + O_2 \rightarrow OH + O$	2.77(-7)	-0.9	-8750	3
8. $OH + OH \rightarrow H_2O + O$	3.5(-16)	1.4	200	3
9. $OH + HO_2 \rightarrow H_2O + O_2$	2.4(-8)	-1	0	3
10. $O + HO_2 \rightarrow OH + O_2$	2.9(-11)	0	200	3
11. $HO_2 + HO_2 \rightarrow O_2 + H_2O_2$	3.32(-12)	0	0	3

[a] 1, Hsu et al.[8] 2, Baulch et al.[4] 3, Tsang and Hampson[15] indicates estimated temperature dependence.

adding a He bypass flow after the water saturator. By varying the ratio of flow through the bubbler and bypass while keeping the total He flow constant, and by changing the bubbler temperature, the H_2O flow could be independently varied.

Hydrogen atoms were produced instantaneously by photolysis of either H_2S or H_2O. In the case of H_2S as precursor, the important chemical reactions which occurred are shown in Table I where the rate coefficient, k, is related to the Arrhenius parameters by

$$k = AT^n \exp(B/T) \quad (3)$$

The time-dependent H atom concentration can be expressed in terms of the rates of these reactions by

$$d[H]/dt = -(k_1[O_2][M] + k_2[H_2S] + k_3[HO_2] + k_6[HS] + k_7[O_2])[H] + k_4[O][HS] \quad (4)$$

For negligible H atom production from O + HS (reaction 4) and H atom reaction with the HO_2 product (reaction 3), the slope of a plot of ln[H] vs time gives the effective first-order decay rate, k':

$$k' = (k_1[M] + k_7)[O_2] + k_2[H_2S] + k_6[HS] \quad (5)$$

Measuring the first-order decay rates as a function of $[O_2]$ yields the second-order decay rate coefficient, k''

$$k'' = k_1[M] + k_7 \quad (6)$$

Finally, measuring a series of second-order decay rate coefficients as a function of pressure ([M]) yields the desired third-order rate coefficient, $k''' = k_1$. This experimental procedure was used to measure the three-body rate coefficient.

Modeling studies using a chemical kinetics differential equation program were used to select operating conditions where secondary chemistry (such as H atom production or secondary reactions with HO_2) was minimal. As in previous studies, the influence of secondary chemistry on the measured decay rates could not be completely eliminated.[7,8] Its importance increased at higher temperatures, where oxygen absorption of the 193-nm photolysis laser resulted in increased O atom production. As will be discussed, the measured rate coefficients were corrected for the appropriate secondary chemistry (Table I or Table II) over the range of reactant concentrations, temperatures, and pressures used in the experiments. These corrections were never more than 10%.

The important chemical reactions for the H_2O system are similar to those for the H_2S chemical system. These reactions are shown in Table II with their kinetic parameters. This reaction set was used to correct the $H + O_2 + H_2O$ rate coefficient measurements for secondary chemistry.

Secondary chemistry effects were examined over a range of molecular concentrations characteristic of the experiments. Number densities of the radicals produced by laser photolysis

TABLE II: Kinetic Parameters for Rate Coefficients Included in H_2O Based Studies of $H + O_2 + H_2O$

	A	n	B	ref[a]
1a. $H + O_2 + He \rightarrow HO_2 + He$	4.0(-33)	0	560	1
1b. $H + O_2 + H_2O \rightarrow HO_2 + H_2O$	1.9(-32)	0	1050	1
1c. $H + O_2 + O_2 \rightarrow HO_2 + O_2$	6.5(-33)	0	680	1
2. $H + H_2O \rightarrow H_2 + OH$	1.0(-16)	1.9	-9265	2
3. $H + HO_2 \rightarrow OH + OH$	3.6(-10)	0	-503	2
4. $O + OH \rightarrow O_2 + H$	7.5(-10)	-0.5	-30	2
5. $O + H_2O \rightarrow OH + OH$	7.6(-15)	1.3	-8605	2
6. $H + OH \rightarrow H_2 + O$	8.1(-21)	2.8	-1950	2
7. $H + OH + M \rightarrow H_2O + M$	6.1(-26)	-2.0	0	2
8. $H + O_2 \rightarrow OH + O$	2.8(-7)	-0.9	-8750	2
9. $OH + OH \rightarrow H_2O + O$	3.5(-16)	1.4	200	2
10. $OH + HO_2 \rightarrow H_2O + O_2$	2.4(-8)	-1	0	2
11. $O + HO_2 \rightarrow OH + O_2$	2.9(-11)	0	200	2
12. $HO_2 + HO_2 \rightarrow O_2 + H_2O_2$	3.32(-12)	0	0	2

[a] 1, Hsu et al.[8] 2, Tsang and Hampson.[15]

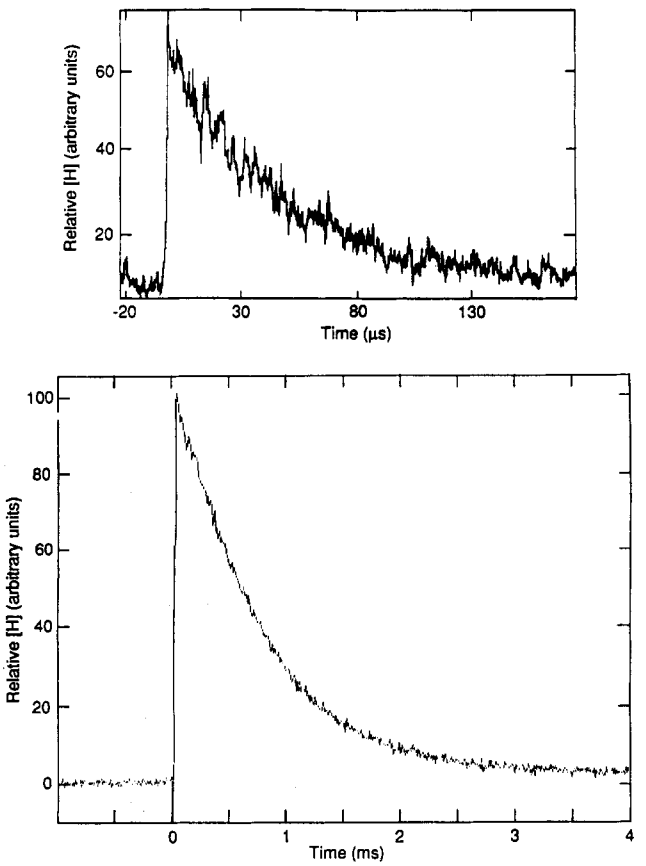

Figure 3. Time-dependent H atom concentration following photolysis of H_2S. (a) LIF probing of H atoms for 216 Torr of N_2 and 3 Torr of O_2 at 298 K. (b) Lyman-α resonance absorption detection of H atoms for 255 Torr of N_2 and 0.5 Torr of O_2 at 298 K.

were determined from the laser fluence, the number density of the precursor molecule, and their absorption cross sections. The temperature-dependent cross sections are

$$\sigma(H_2S)^{16} = 6 \times 10^{-18} \text{ cm}^{-2} \text{ molecule}^{-1}$$

$$\sigma(O_2)^{17} = \exp(-39.4 - 6404.2/T + 985045.5/T^2)$$

$$\sigma(H_2O)^{10} = \frac{2 \times 10^{-21} + 2 \times 10^{-18} \exp(-5400/T)}{1 + \exp(-5400/T)} \quad (7)$$

3. Results

Sample time-resolved H atom signals are shown in Figure 3 for both the LIF and the Lyman-α resonance absorption

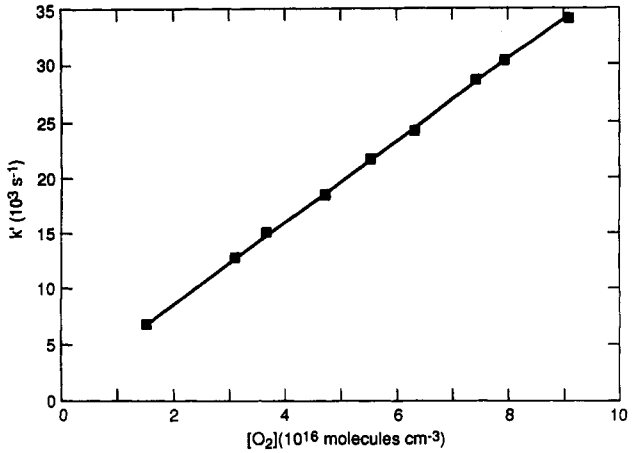

Figure 4. H atom decay rates as a function of oxygen concentration for M = N_2. Lyman–α resonance absorption detection of H atoms at 250 Torr and 298 K. Second-order rate coefficient is (3.71 ± 0.06) × 10^{-13} cm^3 $molecule^{-1}$ s^{-1}.

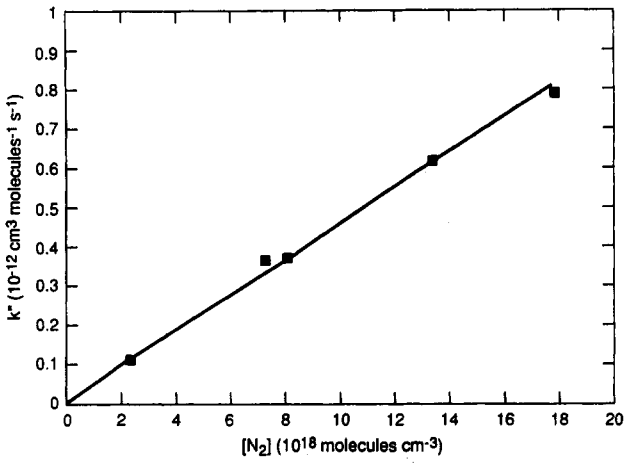

Figure 5. Second-order H atom decay rate coefficients as a function of total pressure for H + O_2 + N_2 at 298 K. The three-body rate coefficient measured by Lyman–α detection is (4.6 ± 0.3) × 10^{-32} cm^6 $molecule^{-2}$ s^{-1}.

measurements. As discussed above, the signal-to-noise ratio of the resonance absorption studies is superior because the entire time-dependent H atom signal was measured on every laser pulse, eliminating uncertainties introduced by drifts in the probe laser power. These exponential decays were fit using a least-squares method to obtain the H atom decay rate, k'. This decay rate was measured for a series of oxygen concentrations. A Stern–Volmer plot of decay rate vs $[O_2]$ yields the second-order rate coefficient as shown in Figure 4. (Note: All quoted errors are 2σ statistical error limits based on least-squares fitting of the data. Systematic errors are estimated to be 10% of the measured rate coefficients.)

3.1. Temperature-Dependent Three-Body Rate Coefficients for N_2. The second-order rate coefficients were measured for a variety of total pressures to yield the three-body rate coefficients. This rate coefficient was measured for N_2 as a third body by both LIF and resonant Lyman–α absorption. Sample room-temperature data for Lyman–α absorption are shown in Figure 5 and the temperature-dependent data are summarized in Table III. The highest temperature at which N_2 three-body rate coefficients were measured was 580 K. Efforts to make measurements at higher temperatures were complicated by increased production of O atoms. The importance of competing reactions such as O + HS was evident from the nonlinear second-order plots.

Modeling studies were performed to assess the possible complications of secondary chemistry on the Lyman–α kinetic rate coefficient measurements. A chemical integration code was used to generate time-dependent H atom concentrations from

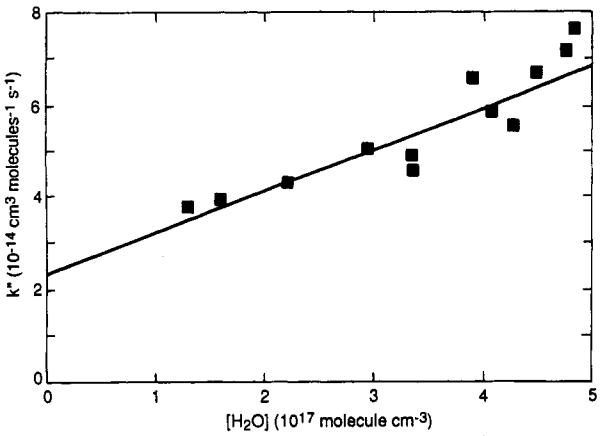

Figure 6. Second-order H atom rate coefficients as a function of H_2O concentration for H + O_2 + H_2O at 650 K. The three-body rate coefficient measured is (0.91 ± 0.3) × 10^{-31} cm^6 $molecule^{-2}$ s^{-1}.

TABLE III: Summary of Three-Body Rate Coefficients for H + O_2 + N_2 Measured by Lyman–α Resonance Absorption and Laser-Induced Fluorescence (LIF)

	three-body rate coeff, 10^{-32} cm^6 $molecule^{-2}$ s^{-1}	
temp, K	Lyman–α	LIF
298	4.6 ± 0.3	4.0 ± 0.6
470	1.73 ± 0.06	
550		1.2 ± 0.3
580	1.1 ± 0.2	

initial reactant concentrations and the reactions given in Table I. The initial concentrations were chosen to cover the range employed in the actual experiments. The H atom decays were then fit as a function of oxygen concentration and total pressure to determine the three-body rate coefficient. The final model-derived three-body rate coefficient was then compared with the rate coefficient input into the model to quantify the secondary chemistry perturbations. For the highest temperature (580 K) Lyman–α measurements, where O atom induced secondary chemistry would be largest, the modeling gave a derived rate coefficient which was 6% smaller than that which was input into the model. This error is less than the experimental error limits suggesting that secondary chemistry had a minimal effect on the Lyman–α kinetic measurements performed.

The LIF and Lyman–α measurement techniques give results which agree quite well. The room-temperature LIF rate coefficient value is slightly lower than the Lyman–α result but agrees within the combined 2σ statistical error bars listed. The Arrhenius expression for the three-body rate coefficient determined from a combination of the Lyman–α and LIF data is

$$k'''(N_2) = (2.9 \pm 0.8) \times 10^{-33} \exp[(825 \pm 130)/T] \quad (8)$$

3.2. Room-Temperature Three-Body Rate Coefficient for Argon. Measurements of the room-temperature three-body rate coefficient for argon were made using LIF to provide additional comparison of our flash photolysis measurement technique with other studies. The data give a rate coefficient of (2.1 ± 0.2) × 10^{-32} cm^6 $molecule^{-2}$ s^{-1}.

3.3. Temperature-Dependent Three-Body Rate Coefficients for H_2O. Measurements of the three-body rate coefficient for H + O_2 + H_2O were performed using LIF detection at three temperatures: 575, 650, and 750 ± 20 K. Measurements were not made at room temperature because of the necessity of heating the walls to minimize condensation and achieve the high water concentrations required. Sample data at 650 K are shown in Figure 6.

Modeling was used to determine the perturbations from secondary chemistry for the experimental operating conditions employed in the H_2O experiments. The corrections for 575 and

TABLE IV: Summary of Experimentally Measured Three-Body Rate Coefficients for H + O_2 + H_2O and Rate Coefficients Corrected for Secondary Chemistry

	three-body rate coeff, 10^{-31} cm^6 molecule^{-2} s^{-1}	
temp, K	exptl	corrected
575	1.2 ● 0.2	1.2 ± 0.3
650	0.9 ± 0.3	1.0 ± 0.3
750	1.2 ± 0.3	$1.2^{+0.9}_{-0.6}$

TABLE V: Summary of Intercepts from Second-Order Rate Coefficients Plots in Comparison with Measurements of Hsu et al.[8]

temp, K	[He], atoms cm^{-3}	k'''_{He} (Hsu et al.), cm^6 molecule^{-2} s^{-2}	$k_3'''_{He}$[He], cm^3 molecule^{-1} s^{-1}	second-order intercept
575	1.6×10^{18}	1.06×10^{-32}	1.7×10^{-14}	1.1×10^{-14}
650	1.69×10^{18}	9.47×10^{-33}	1.6×10^{-14}	2.3×10^{-14}
750	1.83×10^{18}	8.4×10^{-33}	1.5×10^{-14}	1.8×10^{-14}

650 K were less than 1% and 8%, respectively. However, the effect of secondary chemistry at 750 K was large since the modeled three-body decay curve was very nonlinear. It is difficult to determine the appropriate correction at this temperature where the measured rate coefficient is less reliable. This uncertainty is expressed in the large error bars for this value. The measurements and corrected values are summarized in Table IV.

The intercepts from the second-order plots vs [H_2O] correspond to the rate coefficient for the H + O_2 + He reaction, k'''_{He}, multiplied by the He concentration. The intercept values are compared with the measurements of k'''_{He} by Hsu et al.[8] in Table V. The intercepts agree within 50% of the value determined from k'''_{He}[He]. Since Hsu's k'''_{He} error bars are ±30%, this agreement seems quite good.

One noticeable difference for the H_2O studies in comparison with the N_2 three-body experiments was a fast reaction which removed H atoms with no O_2 present. The H atom decays were first order, and the decay rate was quadratic in pressure and decreased with temperature. Since this reaction determined the zero oxygen intercept of the first-order decay rate plots for a given temperature, the pressure was reduced to a value at which reasonable decay rates with added O_2 could be measured on top of this background reaction (100–150 Torr). The temperature and pressure dependences suggest that this background reaction might be a three-body process. However, since decay rates of species such as OH did not have the same fast time-dependent behavior, the reaction is not H + OH + M. The decay rates were also much faster than those predicted from the two-body reaction of H and H_2O to produce H_2 and OH. Since the only species present were H_2O, He, and the photolysis products (H and OH), a possible explanation is that the reaction involves a three-body association process between H and H_2O. Subsequent experiments which monitored OH decay rates suggested that the H which rapidly associates with H_2O is still chemically active and available to react in a H atom like manner. The rate coefficient for the association reaction was not measured in the current work.

4. Discussion

A comparison of the current results for H + O_2 + N_2 with other measurements and compilations is summarized in Figure 7. Table VI compares room-temperature rate coefficients measured in this work with other measurements. Our value is less than the discharge flow measurements of Hsu[7] but agrees with the more recent recommendation of Baulch.[5] Our results also agree (within the combined error bars) with previous flash photolysis measurements which used CH_4 as the photochemical precursor for atomic hydrogen.[18,19] Agreement is also excellent between our room-temperature measurements of H + O_2 + Ar and previous flash photolysis measurements.

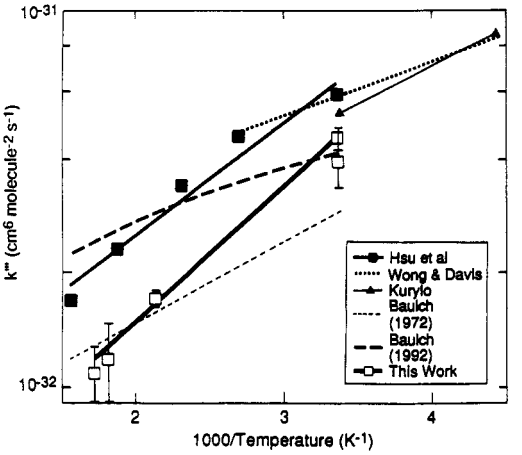

Figure 7. Comparison of recent measurements of the three-body rate coefficient of H + O_2 + N_2.

TABLE VI: Comparison of H + O_2 + M Rate Coefficients at Room Temperature

	three-body rate coeff, 10^{-32} cm^6 molecule^{-2} s^{-1}	
study	M = N_2	M = Ar, He
Baulch et al., 1972[4]	2.9 ± 1.5	2.2 ± 1.1
Kurylo, 1972[18]	5.3 ± 0.8	1.6 ± 0.3
Wong and Davis, 1974[19]	5.5 ± 0.7	2.0 ± 0.23
Hsu et al., 1987[7]	6.0 ± 0.9	2.6 ± 0.2
Baulch et al., 1992[5]	4.0 ± 2.0	1.8 ± 0.9
this work, 1992	4.6 ● 0.3	2.1 ● 0.2

While the room-temperature N_2 and Ar data agree quite well with previous work, the temperature dependences of the three-body rate coefficient vary as shown in Figure 7. These comparisons are complicated by the fact that measurements have been performed in different temperature regimes. We can compare Arrhenius expressions for our results with Hsu et al. since their data were taken over comparable temperature ranges. The expressions are

this work

$$k''' = (2.9 \pm 0.8) \times 10^{-33} \exp[(825 \pm 130)/T]$$

Hsu et al.[8]

$$k''' = (6.5 \pm 2.2) \times 10^{-33} \exp[(680 \pm 100)/T] \quad (9)$$

While the temperature dependence of these two measurements are consistent, the overall magnitudes of the rate coefficients differ by approximately a factor of 2.

The factor of 2 difference in our higher temperature results with the results of Hsu et al. is surprising in light of the excellent agreement of the room-temperature argon data and the high-temperature H_2O data (see below) of these two studies. While Hsu et al.'s results do agree with previous room-temperature results within the combined error bars (as do ours), they seem to be on the high side of many of these measurements. These careful experiments were performed at rather high pressures for a flow tube reactor, but it is uncertain if this caused any systematic errors. It is interesting to note that our high-temperature values are more in line with the 1972 recommendations of Baulch et al.,[4] while the larger rate coefficient measurements of Hsu et al. may be reflected in the increased values recommended in the most recent Baulch et al. review.[5] The resulting temperature dependence of this review seems significantly different from both this work and that of Hsu et al. and may therefore be in question.

Most of the high-temperature rate coefficient measurements have been performed in shock tube or flame studies using

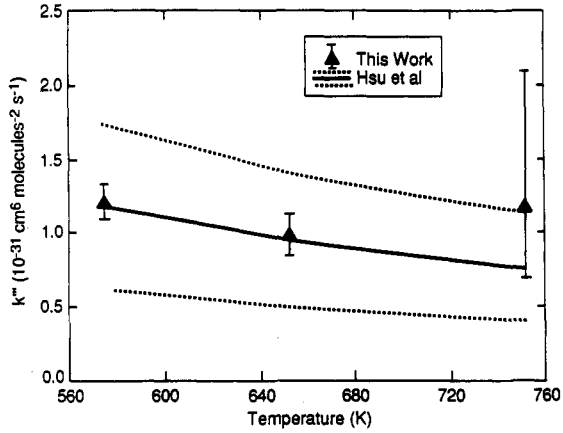

Figure 8. Comparison of measurements of the three-body rate coefficient for $H + O_2 + H_2O$ of this work and that of Hsu et al.[8]

argon.[20-24] However, Slack measured the rate coefficient with nitrogen in a shock tube study to be $(9.1 \pm 1.6) \times 10^{-33}$ cm^6 molecule^{-2} s^{-1} for an estimated temperature of 980–1176 K.[25] This value agrees with the temperature-extrapolated values of both this work and Hsu et al. within the error bars of the measurements.

Comparison of H_2O Three-Body Rate Coefficients. The three-body rate coefficient for water measured in this work and that of Hsu et al.[8] were performed over the same temperature range. These results are compared in Figure 8. For the temperatures at which secondary chemistry is minimal, the two measurement techniques are in excellent agreement, within a few percent. A weighted least-squares fit to our data gives the following Arrhenius expression:

$$k(H_2O) = (3.9 \pm 3.1) \times 10^{-32} \exp[(600 \pm 1050)/T] \quad (10)$$

This can be compared with the Arrhenius expression of Hsu et al.[8]

$$k(H_2O) = (1.9 \pm 0.9) \times 10^{-32} \exp[(1050 \pm 140)/T] \quad (11)$$

While secondary chemistry complications in the highest temperature data produce large error bars in our temperature dependence, we can extrapolate our data for comparison with other rate coefficient measurements. At 1500 K, flame studies of Dixon-Lewis and Williams[26] give a value of 2.2×10^{-32} cm^6 molecule^{-2} s^{-1}, while the shock tube work of Getzinger and Schott[20] gives a value of 1.2×10^{-31} cm^6 molecule^{-2} s^{-1}. This can be compared to a value of 3.8×10^{-32} cm^6 molecule^{-2} s^{-1} extrapolated from Hsu et al.'s results and 6×10^{-32} cm^6 molecule^{-2} s^{-1} extrapolated from our data. Unfortunately, the large error bars on our results encompass the values of both Dixon-Lewis and Williams and Getzinger and Schott.

5. Conclusions

Three-body rate coefficients have been measured using a high-temperature flash photolysis reactor to quantify the three-body rate coefficients of $H + O_2 + M$ for M = N_2, Ar, and H_2O. The rate coefficient for N_2 is $k''' = (2.9 \pm 0.8) \times 10^{-33} \exp[(825 \pm 130)/T]$. This result agrees well with previous low-temperature flash photolysis studies as well as the high-temperature shock tube studies of Slack. However, it gives consistently smaller values than the recent discharge flow results of Hsu et al. although the temperature dependence measured in these two studies is in good agreement. The rate coefficient with Ar at 298 K is $(2.1 \pm 0.2) \times 10^{-32}$ cm^6 molecule^{-2} s^{-1}, which agrees well with previous work. The three-body rate coefficient measurements for $H + O_2 + H_2O$ are in excellent agreement with the recent measurements of Hsu et al. at temperatures less than 700 K where secondary chemistry does not complicate the experimental measurements. With the exception of the temperature dependence of the $H + O_2 + N_2$ reaction, these results are consistent with the recommended rate coefficient values currently in use by the combustion community.[5]

Acknowledgment. This work was supported by the NASA Lewis Research Center under Contract No. NAS3-26058, Martin Rabinowitz, Contract Monitor. We thank Drs. Lawrence G. Piper and W. Terry Rawlins at Physical Sciences Inc. for their helpful comments and technical review of this work.

References and Notes

(1) Harradine, D.; Lyman, J.; Oldenborg, R.; Schott, G.; Watanabe, H. AIAA-88-2713, June 1988.
(2) Dixon-Lewis, G. *Combust. Sci. Technol.* **1983**, *34*, 1–29.
(3) Levitt, B. P. *Physical Chemistry of Fast Reactions*; Plenum Press: New York, 1973; Vol. 1.
(4) Baulch, D. L.; Drysdale, D. D.; Horne, D. G.; Lloyd, A. C. *Evaluated Kinetic Data for High Temperature Reactions*; CRC Press: Boca Raton, FL, 1972; Vol. 1.
(5) Baulch, D. L.; Cobos, C. J.; Cox, R. A.; Esser, C.; Frank, P.; Just, Th.; Kerr, J. A.; Pilling, M. J.; Troe, J.; Walker, R. W.; Warnatz, J. *J. Phys. Chem. Ref. Data* **1992**, *21* (No. 3), 1992.
(6) Chemical Kinetic and Photochemical Data for Use in Stratospheric *Modelling*. Evaluation Number 9: NASA Panel for Data Evaluation, 1990.
(7) Hsu, K.-J.; Durant, J. L.; Kaufman, F. *J. Phys. Chem.* **1987**, *91*, 1895.
(8) Hsu, K.-J.; Anderson, S. M.; Durant, J. L.; Kaufman, F. *J. Phys. Chem.* **1989**, *93*, 1018.
(9) Davidson, D. F.; Chang, A. Y.; Kohse-Höinghaus, K.; Hanson, R. K. *J. Quant. Spectrosc. Rad. Transfer* **1989**, *42*, 267.
(10) Kessler, W. J.; Carleton, K. L.; Marinelli, W. J. *J. Quant. Spect. Rad. Transfer*, submitted.
(11) Hänsch, T. W., Lee; S. A.; Wallenstein, R.; Wieman, C. *Phys. Rev. Lett.* **1975**, *34*, 307.
(12) Bokor, J.; Freeman, R. R.; White, J. C.; Storz, R. H. *Phys. Rev. A* **1981**, *24*, 24.
(13) Lucht, R. P.; Salmon, J. T.; King, G. G.; Sweeney, D. W.; Laurendeau, N. M. *Opt. Lett.* **1873**, *8*, 365.
(14) Wiese, W. L.; Smith, M. W.; Glennon, B. M. National Standard Reference Data Series National Bureau of Standards 4 (Category 3), Issued May 29, 1966.
(15) Tsang, W.; Hampson, R. F. *J. Phys. Chem. Ref. Data* **1986**, *15* (3), 1087.
(16) Watanabe, K.; Jursa, A. S. *J. Chem. Phys.* **1964**, *41*, 1650.
(17) Lee, M. P.; Hanson, R. K. *J. Quant. Spect. Radiat. Transf.* **1986**, *36*, 425.
(18) Kurylo, M. J. *J. Phys. Chem.* **1972**, *76*, 3518.
(19) Wong, W.; Davis, D. D. *Int. J. Chem. Kinet.* **1974**, *1*, 401.
(20) Getzinger, R. W.; Schott, G. L. *J. Chem. Phys.* **1965**, *43*, 3237.
(21) Blair, L. S.; Getzinger, R. W. *Combust. Flame* **1970**, *14*, 5.
(22) Fenimore, C. P.; Jones, G. W. Sympos. (Int.) Combustion [Proc.], 10th, 489, 1965.
(23) Gutman, D.; Hardwidge, E. A.; Dougherty, F. A.; Lutz, R. W. *J. Chem. Phys.* **1967**, *47*, 4400.
(24) Pirraglia, A. N.; Michael, J. V.; Sutherland, J. W.; Klemm, R. B. *J. Phys. Chem.* **1989**, *93*, 282.
(25) Slack, M. W. *Combust. Flame* **1977**, 241.
(26) Dixon-Lewis, G.; Williams, A. Sympos. (Int.) Combustion [Proc.], 11th, 951, 1967.